This is the Submitted version (post-print) of the following paper: PEG-crosslinked-chitosan hydrogel films for in situ delivery of Opuntia ficus-indica extract by Catanzano et al. published on Carbohydrate Polymers 264 (2021) 117987, DOI: https://doi.org/10.1016/j.carbpol.2021.117987. The final published version is available on the publisher website

PEG-CROSSLINKED-CHITOSAN HYDROGEL FILMS FOR IN SITU DELIVERY OF OPUNTIA FICUS-INDICA EXTRACT

O. Catanzano [a] 1, G. Gomez d'Ayala [a] 1, A. D'Agostino [b], F. Di Lorenzo [c], C. Schiraldi [b], M. Malinconico [a], R. Lanzetta [c], F. Bonina [d], P. Laurienzo [a]

[a] *Institute for Polymers, Composites and Biomaterials (IPCB) – CNR, Via Campi Flegrei 34, Pozzuoli, Naples, Italy*

[b] *Department of Experimental Medicine, School of Medicine, University of Campania "Luigi Vanvitelli", Via L. De Crecchio 7, 80138 Naples, Italy*

[c] *Department of Chemical Sciences, University of Naples "Federico II", Complesso Universitario Monte S. Angelo, Via Cinthia 4, 80126 Naples, Italy*

[d] *Department of Drug Sciences, University of Catania, Viale Andrea Doria 6, 95125 Catania, Italy*

Received 1 July 2020, Revised 29 January 2021, Accepted 23 March 2021, Available online 26 March 2021, Version of Record 5 April 2021.

Abstract

In the present study, chitosan-based wound dressings loaded with the extract of Opuntia ficus-indica (OPU) were prepared. OPU is known for its capability to accelerate skin injury repair. Chitosan (Ch) was crosslinked with a low molecular weight diepoxy-poly(ethylene glycol) (diePEG), and hydrogel films with different Ch/PEG composition and OPU content were prepared by casting. The occurrence of crosslinking reaction was confirmed by FTIR spectroscopy. FTIR and DSC analysis suggested that ionic interactions occur between chitosan and OPU. Tensile tests evidenced that the crosslinking caused a decrease of Young's modulus, which approaches the value of the human skin modulus. Swelling characteristics, water vapor transmission rate, and release kinetics demonstrated that these films are adequate for the proposed application. Finally, a scratch test on a keratinocytes monolayer showed that the rate of cell migration in the presence of OPU-loaded samples is about 3-fold higher compared to unloaded films, confirming the repairing activity of OPU.

Highlights

• Opuntia ficus-indica (OPU) extract was loaded within PEG- crosslinked chitosan films.

• The prepared films showed swelling and vapor transmission rate suitable as wound dressings.

• At a given composition, the Young's modulus of films is close to that of human skin.

• Release of OPU was higher from films at low OPU load.

• Low OPU content films showed the best tissue repairing activity.

1. Introduction

The extract of Opuntia ficus-indica (OPU), a member of Cactacae family, was widely used in folk medicine for the treatment of skin and epithelium wound burns, edema, hyperlipidemia, obesity, and catarrhal gastritis (Rocchetti, Pellizzoni, Montesano, & Lucini, 2018). This extract has become very popular in recent years due to a series of evidences that confirms its activity on wound healing by accelerating the re-epithelization and remodeling phases (Panico et al., 2007; Trombetta et al., 2006). Furthermore, if applied to full-thickness skin defects in a rabbit ear wound model, OPU has proven to decrease the formation of hypertrophic scarring (Fang, Huang, You, & Ma, 2015). These characteristics make OPU attractive as a component for active wound dressing formulation, but still now no examples of delivery devices for local release of OPU can be found in literature. Wound dressings are traditionally used to protect the wound from external contamination, but more recently the progress in wound management also requires their use as platforms to deliver bioactive molecules directly to the site (Boateng & Catanzano, 2015) and as support for healing. In particular, there is interest in achieving a fast wound closure in order to minimize the possibility of infection and/or chronicity of wounds. Chitosan (Ch) is a natural polymer that can play a positive role in all of the steps that lead to the healing of a wound injury. (Yang et al., 2008). Chitosan is a natural amino-polysaccharide derived from chitin, known as the second most abundant natural polysaccharide after cellulose (Oyatogun et al., 2020). It is commercially available in a wide variety of molecular weights, from oligomers to high-molecular-weight polymers. Both the deacetylation degree (DD) and molecular weight influence the chemistry, solubility and biological activities of chitosan. Chitosan is extensively used in the preparation of films for wound delivery of bioactive molecules due to its significant biological properties such as biocompatibility, biodegradability, low toxicity, and most importantly antimicrobial, antioxidant and wound healing properties (Boateng & Catanzano, 2015; Elgadir et al., 2015; Matica, Aachmann, Tondervik, Sletta, & Ostafe, 2019;

Mengatto, Helbling, & Luna, 2012). Moreover, when applied on an open wound, chitosan exerts a strong haemostatic action, which leading to the development of a series of haemostatic patches and gels (Hemcon®) that are already available on the market. Nevertheless, the main drawback in the scaling-up of chitosan applications in the biomedical field is represented by the poor long-term stability of chitosan-based pharmaceutical products (Szymanska & Winnicka, 2015). Furthermore, chitosan films are rigid and brittle, thus not useful for the fabrication of biomedical devices, as artificial scaffolds or dressings. On the other hand, hydrogel films based on crosslinked chitosan are flexible and expected to be applicable for some biomedical devices (Kiuchi, Kai, & Inoue, 2008). The purpose of this work is to prepare an advanced wound dressing based on chitosan for local delivery of Opuntia extract, in order to help the physiologic wound healing process. The integration of an active ingredient into a polymeric dressing is a strategy increasingly used in wound healing to obtain an *in situ* delivery with a fine control of the release rate. To increase stability and also improve mechanical properties, chitosan was crosslinked with diepoxy-poly(ethylene glycol) (diePEG). PEG is largely used in biomedical devices thanks to its hydrophilicity, absence of cytotoxicity and excellent tissue biocompatibility (Ivanova, Bazaka, & Crawford, 2014). Hydrogel films with different chitosan/PEG ratio crosslinked in an aqueous solution and loaded with various amounts of OPU were prepared. Chemical and physico-chemical characteristics of blank and OPU loaded films were evaluated by several techniques to assess the structure and test their performance for wound dressing applications. The release of OPU from the various films was investigated, and the repairing activity of the more promising films at different OPU contents was finally evaluated using a simplified in vitro cellular model based on a scratched keratinocytes monolayer.

2. Experimental

2.1. Materials

Chitosan (Ch), crab-shell origin, high viscosity (400 cps 1% in acetic acid, 20 °C; DD 75 %), diepoxyPEG (diePEG, MW =_ _500, epoxy conversion ~ 95÷98 %), sodium chloride, potassium chloride, sodium phosphate dibasic dihydrate, calcium chloride, were purchased from Sigma-Aldrich, Milan, Italy. The *Opuntia ficus-indica* extract (OPU) was supplied by BIONAP srl (OPUNTIA BIOCOMPLEX SH, Piano Tavola Belpasso (CT), Italy) and was obtained by extraction from *Opuntia* cladodes by a mechanical press, heated at 90 °C for 1 h, and then filtered and heated again at 90 °C for 2 h. The obtained clear solution was

decanted to eliminate residual chlorophyll and lyophilized to obtain a powder consisting of small molecular components and high molecular weight polysaccharides (Di Lorenzo et al., 2017). Solubility characteristics of OPU are reported in Table S1. All solvents were of reagent grade with the highest purity available. Deionized ultra-filtered water was used throughout this study. For cell culture, Dulbecco's Phosphate Buffered Saline (DPBS) was purchased from Lonza Sales Ltd., Switzerland (Cat. N. BE17-512 F). Dulbecco's Modified Eagles Medium (DMEM), Fetal Bovine Serum (FBS), penicillin–streptomycin solution (Cat. N. DE17-602E) and fungizone (Cat. N. 17836E) were purchased from Life Technologies (Breda, The Netherlands). Collagen was purchased from Sigma-Aldrich (Milan, Italy). A spontaneously transformed non-tumorigenic human keratinocyte cell line (HaCat cells) was used for *in vitro* scratch-wound-healing assay as previously reported (D'Agostino et al., 2019). Cells were grown in complete medium (DMEM 10 % v/v FBS, Pen/Strep and Fungizone 1 % p/v) on tissue culture plates previously coated with collagen for (Corning Incorporated, New York, NY, USA) in an incubator with a humidified atmosphere (95 % air/5 % CO_2 v/v) at 37 °C.

2.2. Preparation of blank and OPU-loaded films

Blank and OPU-loaded Ch/diePEG crosslinked films were obtained by solvent casting method. 100 mg of chitosan were dissolved in 10 mL of 0,4% acetic acid (1% w/v). Different amounts of diePEG, namely 50, 100 and 200 μL, were added to the chitosan solution by wise dropping and left to react at 80 °C for 24 h under magnetic stirring (the three formulations were coded 1:0.5, 1:1 and 1:2, respectively). During crosslinking reaction, the solution became gradually viscous with formation of a mild hydrogel. The solutions were poured into a plastic petri dish (diameter 10 cm) and left to dry at room temperature under a fume hood for 3 days. The occurrence of reaction was confirmed by FTIR through disappearance of the epoxy ring band at 912 cm^{-1}. To obtain the OPU-loaded hydrogel films, different amounts of lyophilized OPU extract (namely 50, 100 and 200 mg, corresponding to a concentration of OPU of 0.1 %, 0.25 % and 0.5 % w/v, respectively) were added to the Ch/diePEG solutions at the end of the crosslinking reaction. OPU was added in tiny amounts to avoid lump formation. The solutions were left under magnetic stirring until complete dissolution of OPU and then poured into a plastic petri dish and air-dried at room temperature for 3 days, as described above. The films appeared flexible and homogeneous (Supplementary, Fig. S1). After visual examination to identify any physical defects, they were wrapped with aluminum foil and kept in a desiccator until required. The thickness of

the various films was measured by a digital micrometer and reported as the average value of at least ten random points (Table S2). To assess the extent of reaction, unloaded chitosan hydrogel films were subjected to a prolonged washing with water to evaluate eventual leakage of unreacted diePEG. Pre-weighed dried film samples obtained from a 100 mm petri dish were cut in four pieces, placed in a Falcon tube containing 50 mL of water and left on an orbital oscillator overnight. After this time, the films were recovered, dried under vacuum at 50 °C for 24 h and weighed again. The percentage of weight loss for each formulation was calculated using Eq. (1):

$$Weight\ loss\ (\%) = \frac{W_0 - W}{dP_0} \times 100$$

Where W_0 is the mass of the initial dry film, W is the mass of the dry film after washing, and dP_0 is the initial diePEG content. Results are the mean of four independent measurements.

2.3. Attenuated total reflectance Fourier Transform IR spectroscopy (ATR-FTIR)

FTIR spectra were obtained in the attenuated total reflection mode (ATR) using a Perkin-Elmer spectrometer (Norwalk, CT, USA) equipped with universal ATR accessory, fitted with a diamond optical element and ZnSe focusing elements. The apparatus operates with a single reflection at an incident angle of 45°. The analysis was carried out on films at room temperature and ambient humidity. For each spectrum, 32 scans were acquired in the 4000-650 cm^{-1} range, with a resolution of 4 cm^{-1}.

2.4. Thermal analysis

Differential Scanning Calorimetry (DSC) analysis was carried out using a Q2000 calorimeter (TA Instruments). Each sample (about 4 mg) was filled in a sealed aluminum pan. The samples were tested under nitrogen flow (50 mL/min). The following protocol was used: heating from 25 to 120 °C at 10 °C/min rate (I run); isotherm at 120 °C for 1 h; cooling to 25 °C at 20 °C/min rate; heating to 200 °C at 10 °C/min rate (II run). Glass transition temperatures (Tg) were taken in II run.

2.5. Moisture content

The moisture content (MC) in the films was determined by thermogravimetric analysis (TGA, Perkin Elmer Pyris Diamond apparatus). Samples (3–6 mg) were heated at 10 °C/min from 25 to 400 °C under nitrogen flow (50 mL/min). The weight loss in the range between 25 and 120 °C, corresponding to the loss of bounded and absorbed water, was determined using TA Universal Analysis 2000 software, and MC (%) was calculated as the percentage of water removed from the films.

2.6. Tensile properties

Tensile properties of films containing 0.5 % OPU were analyzed on an INSTRON 4444 instrument at room temperature (25 °C) using a 100 N load cell. Films were cut into dumbbell shapes (specimen dimensions: gauge length 28 mm, gauge width 4 mm, total length 40 mm, average thickness 0.1 mm) and mounted using screw jaws with a knurled surface. Their average thickness (measured with a digital caliper in at least 4 different points) was entered into the software program. Tensile tests were run at a crosshead speed rate of 2 mm min^{-1} and each sample was loaded to failure. The results were expressed as the mean value of three independent measurements.

2.7. Swelling

The percentage swelling ratio was determined by placing the films in Phosphate Buffer Saline (PBS, NaCl 120 mM, KCl 2.7 mM, Na_2HPO_4 10 mM, pH 7.4) solution. The initial weight of each sample was accurately recorded using an analytical balance, and then they were placed in a petri dish filled with 2 mL of PBS. The experiment was carried out a room temperature. At fixed time intervals (0.5, 1, 2, 3, 6, 24 and 48 h) the samples were taken out and weighed, after carefully removing the excess of fluids using tissue paper. After every weight measurement, the samples were re-immersed in 2 mL of fresh PBS. The percentage swelling ratio (*SR* %) at each time point was calculated using Eq. (2):

$$SR\ (\%) = \frac{W - W_0}{W_0} \times 100 \qquad (2)$$

Where W is the mass of the swollen sample and W_0 is the mass of the initial dry sample. Assuming that the network swells uniformly in all directions, the equilibrium water content (EWC) can be defined as the ratio between the weight of the swollen sample after 24 h in

water and its initial weight. The equilibrium water content (EWC) percent was calculated by Eq. (3):

$$EWC\ (\%) = \frac{W_e - W_d}{W_e} \times 100 \qquad (3)$$

Where W_e is the mass of the swollen sample at equilibrium and W_d is the mass of the dry sample at equilibrium.

2.8. Water vapor transmission rate

Water vapor transmission rate (WVTR) was measured according to the ASTM E96 wet method (ASTM-International., 2013) using a CEAST metal cup with a 706.5 × _10^{-6} m^2 exposed area. Cups were placed in an environmental chamber set at a temperature of 25 ◦C and a relative humidity of 50 %; each sample was first equilibrated for 48 h before measurements, then weighed every 24 h for 5 days. WVTR values were expressed in g/h· _m_2 and determined with graphic analysis method following Eq. (4):

$$\mathrm{WVTR} = \Delta G / t \times A \qquad (4)$$

where ΔG was the weight change (g), t was the time during which G occurred (h), A was the test area cup (m_2) and ΔG/t was the slope of strains line (g· _h^{-1}). Data are the mean of three measurements.

2.9. OPU release

Release studies were performed using a custom apparatus designed to mimic exudate penetration from the wound bed (Rossi et al., 2007; Straccia, Gomez d'Ayala, Romano, Oliva, & Laurienzo, 2015). This apparatus consists of a glass porous septum placed on the top of a 10 mL beaker filled with PBS solution (Supplementary, Fig. S1). OPU loaded films were placed on the porous septum to be in contact with the release medium only by the lower surface. At scheduled time intervals, 2 mL of the release medium were withdrawn, transferred in a 1 cm quartz cell and analyzed for OPU content. The OPU concentration was quantified by means of UV–vis spectroscopy using a Perkin Elmer Inc. (Waltham, MA, USA)

spectrophotometer with a double beam/single monochromator optical system, measuring the absorbance at 274 nm. Experiments were performed in triplicate. The mean cumulative drug release percentage was calculated using a calibration curve build using OPU solutions in PBS of known concentration (Fig. S2, Supplementary). The linearity of the response was verified over the concentration range of 0.1-0.6 mg/mL (r_2≥0.995).

2.10. Cells culture and biological response

A preliminary experiment to evaluate any influence of the OPU loaded films on the natural wound repair was accomplished using a simple and robust wound healing assay with a slightly modified protocol recently reported in the literature (D'Agostino et al., 2019) Particularly, wound healing assay was performed through a videomicroscopy timelapse (TLVM) station that allows the *on line* monitoring of the gap closure in a simplified wound model based on a scratched cellular monolayer, in the absence (negative control) and in the presence of the films loaded with OPU. The films (Ch/diePEG 1:0.5) were cut with a cylindrical die cutter (Φ _=_ _14 mm) and sterilized by washing with an ethanolic solution (70 % v/v), then with sterile PBS buffer solution containing penicillin/streptomycin (5 % v/v) and finally with sterile de-ionized water. Samples were placed into 12-well microplates and incubated at 37 °C and 5% CO_2 in humidified atmosphere. The concentration of OPU in the medium for the various films is reported in Table S3. Films not loaded with OPU were also tested as a control. Confluent HaCat monolayers, previously growth in 12 well containing complete cell medium (DMEM with 10 % FBS) were scratched with a tip to mimic a simplified injury dermal model. DMEM with lower FBS content (1 % FBS) was used as the culture medium to minimize cell proliferation and observe mainly cell migration. Each sample was tested at least in duplicate, and the negative control for cellular repair was represented by the cell alone without films in DMEM 1 % FBS. Scratched cells were allocated in the stage incubator of the microscopy station, where temperature, air humidity and CO_2 content were constantly monitored and controlled. TLVM allowed to continuously monitor cellular migration through different selected field of view (at least five), until the complete wound closure (48□ _72 h). Successively, the digital photos over time were analyzed using the OKOVISION software (Okolab Srl, Italy) to quantify the cell migration rate in the presence of each sample.

2.11. Statistical analysis

Statistical analyses were undertaken using GraphPad Prism®, version 6.00 (GraphPad Software, La Jolla California USA) using one-way ANOVA test. All experiments were performed in triplicate and the results were expressed as the mean ± _standard deviation (SD). A *p*-values below 0.05 was considered as significant.

3. Results and discussion

3.1. Preparation and preliminary characterization of films

This work describes the development of an advanced wound dressing intended as delivery system for an extract of *Opuntia ficus-indica*. For this purpose, chitosan was crosslinked with diePEG and films with different content of PEG and OPU were prepared. PEG-crosslinked chitosan hydrogel films have been widely investigated in literature (Tanuma, Kiuchi, Kai, Yazawa, & Inoue, 2009, 2010). Here, crosslinking of chitosan was achieved *via* a classical amine-epoxy reaction, carried out following a slightly modified procedure previously reported (Kiuchi et al., 2008). The gelling solution was transferred in a petri dish and left at room temperature for three days until dryness, and shape uniform, transparent films were obtained. (Supplementary, Fig. S3). On the contrary, it was found that keeping the solution in a sealed dish at 80 °C for further 24 h leads to the formation of non-uniform films, unlike what was reported by Kiuchi et al. The occurrence of the reaction between diepoxy-PEG and chitosan was confirmed by FTIR spectroscopy (Fig. 1). According to the scheme of reaction reported in Fig. S4, the amine-epoxy reaction caused the opening of the epoxy ring of diePEG. As a consequence, the complete disappearance of the C–OC– _bending vibration at 912 cm^{-1} specific of the epoxy ring is a clear signal of the full reaction of diepoxy end groups of diePEG, with formation of a chemically crosslinked Ch/diePEG network. As a further confirmation, every attempt to dissolve the crosslinked films in various solvents, as acetic acid, has failed. PEG is a cytocompatible polymer that does not cause adverse reactions when released to the wound media (Chen et al., 2018). However, the leakage of PEG from the dressing is still undesirable, as it may cause changes in the hydrophilic properties of the material. A leakage test with water was carried out on blank films to estimate any loss of soluble material (mainly, unreacted diePEG or unmodified PEG diol). Unloaded films were shaken in water for 24 h. The results (shown in Fig. 1) demonstrated that films possess very good stability, as the leakage from the dressings did not exceed 2 % of the original diePEG amount. It is worth to note that the material loss % was close to the amount of residual PEG diol in the diePEG product, as reported by the

supplier (see *Materials* section). As a matter of fact, the loss % is independent of the PEG composition in the film. It is therefore reasonable to attribute the weight loss to unmodified PEG diol. In conclusion, the results of FTIR analysis and leakage test account for a quantitative reaction of epoxy end groups of diePEG with chitosan amines. Blank and OPU-loaded films were characterized by several techniques, to highlight the occurrence of physical interactions between the components and to evaluate their performance as potential wound dressings. A non-crosslinked film of chitosan either pure or loaded with the various OPU % was also analyzed as a blank throughout the work.

3.2. FTIR analysis

FTIR spectra of Ch and Ch/diePEG films are reported in Fig. 2a, with the assignment of diagnostic peaks. The bands in the 3600-3000 cm^{-1} region relative to O–H and NH– _stretching vibrations are broad, indicating that hydroxyl and amine groups are involved in intra- and intermolecular hydrogen bonds. The peak at 3266 cm□1 (NH– _stretching vibration of primary amines) decreased regularly at increasing content of diePEG, confirming the reaction of amines with epoxy groups. Accordingly, the NH_2 bending vibration band centered at 1542 cm^{-1} decreased in Ch/diePEG films. The peak at 1633 cm^{-1} is correlated to the residual N-acetyl group from chitin (C– _– _O stretching of amide I). The small band at 1732 cm□1, absent in the spectrum of diePEG, indicates the presence of carbonyl groups, likely originating from slight degradation phenomena (Krauklis & Echtermeyer, 2018). Bands in the range 1400-1250 cm^{-1} are attributed to C–O and COC— _stretching of saccharides units and PEG chains. Films containing 0.5 % OPU show notable changes in the region relative to NH_2 bending vibration (Fig. 2b). In the spectrum of Ch containing 0.5 % OPU, the NH_2 band is broader, indicating interactions of amines with carboxylic acid components of OPU extract. In crosslinked films the band gradually splits at increasing diePEG content. The emerging peak at 1598 cm-1 can be assigned to the $–NH^{3+}$ bending vibration (Ivanova & Spiteller, 2010), confirming the ionic interaction of residual amines of Ch with carboxylic acids of OPU.

3.3. DSC analysis and moisture content

Glass transition (Tg) of chitosan was evaluated by DSC analysis. Both unloaded and OPU-loaded films were analyzed and compared to evaluate the influence on Tg of the different crosslinking degree and OPU loading. It is well known that crosslinking affects the Tg;

moreover, changes in Tg values are also indicative of the establishment of physical interactions between the components at a molecular level. Tg values were taken in the second run, following an isotherm at 120 °C to remove water (Table 1. Representative DSC curves are reported in supplementary material, Fig. S5). Ch shows a Tg at 145 °C, in agreement with literature data (Dong, Ruan, Wang, Zhao, & Bi, 2004). A slight decrease of Tg with respect to free Ch was found for Ch/diePEG 1:0.5 and 1:1, indicating that the addition of flexible PEG chains as crosslinkers results in enhanced chain mobility. Furthermore, the decrease of the number of amines, as a consequence of chemical bonds with diePEG, also contributes to reduce Tg by decreasing inter- and intra-molecular hydrogen bonds between chitosan chains. On the contrary, an increase of Tg was found for 1:2 composition. Thus, in the case of a higher crosslinking degree, the formation of a dense chemical network prevails over the insertion of PEG segments, resulting in Tg increase as normally found upon crosslinking. Addition of OPU did not affect Tg significantly. Nevertheless, a trend of Tg to increase at increasing OPU content could be noticed, supporting the assumption of formation of ionic interactions between dicarboxylic acids of OPU and free amines of Ch, that results in reduced chain mobility. Finally, DSC analysis of OPU extract in form of powder showed a Tg at 92 °C, attributed to the high molecular weight polysaccharides fraction, and an endotherm at 173 °C, corresponding to melting of the low molecular weight components. The endotherm was visible only in the thermogram of Ch + OPU 0.5 % (Fig. S5), whereas it was absent in the crosslinked films, pointing out that the low molecular weight molecules are in an amorphous state when dispersed in the crosslinked polymeric matrices. In general, crystallization inhibition of active ingredients is important to maintain drug solubility and bioavailability, and crystallization inhibitors are often introduced as excipients in solid dosage forms. It is reported in literature that polymers able to form intermolecular interactions with the target compound can form a stable amorphous solid dispersion (Christina, Taylor, & Mauer, 2015). Thus, PEG-crosslinked chitosan is believed to act as a crystallization inhibitor towards low molecular weight components of OPU. This is an important aspect and will be a matter of further study in the future. Moisture content (MC) was studied to understand how the affinity of chitosan-based films to water was influenced by the OPU addition and the crosslinking with different PEG concentrations. Only films with higher OPU content (0.5 %) were analyzed. MC was found to decrease at increasing PEG amounts in the case of blank films, despite the presence of the high hydrophilic PEG (Table 1). This behavior is a consequence of the crosslinking reaction, in which the amines of chitosan are covalently bonded to the epoxy groups of PEG.

Consequently, chitosan becomes less available to bind water molecules, as hydrophilic sites along chains decrease, resulting in lower values of MC. The addition of OPU leads to a slight increase of MC for crosslinked films, due to the introduction of hydrophilic molecules, whereas a decrease was found for not crosslinked chitosan. Analogously to what happens in the case of crosslinking, amines are engaged in ionic interactions with OPU and no more available to bind water.

3.4. Tensile properties

Crucial parameters for wound healing materials are flexibility and elasticity since they determine the conformability of the dressings (*i.e.*, their ability to repeat the shape of the treated tissue) (Thomas & Uzun, 2019). A preliminary evaluation of mechanical properties was carried out by tensile tests on films loaded with the various OPU %, and results are summarized in Table 2. A film of Ch loaded with 0.5 % OPU was also analyzed for comparison. Tensile strength (σ_B) was quite low for all the samples, but still in the range of 2.5–16 MPa reported for the skin (Wang, Khor, Wee, & Lim, 2002). The tensile strength is an important parameter to evaluate the handling of materials. For a wound dressing, this parameter is of particular importance as its easy application on a wound site directly depends on the handling properties (Archana, Singh, Dutta, & Dutta, 2013; Boateng & Catanzano, 2015; Boateng, Matthews, Stevens, & Eccleston, 2008). Elongation at break is higher with respect to non-crosslinked Ch and increased regularly at increasing diePEG amount (up to around 70 % for 1:2 composition). This effect is related to the partial substitution of hydrogen bonds among Ch chains with PEG crosslinks, that reduce chain stiffness. Young modulus (E) decreased considerably at increasing PEG content, particularly in the case of Ch/diePEG 1:1 and 1:2, due to the introduction of a large amount of soft PEG segments and to the strong reduction of hydrogen bonds between chitosan chains. Interestingly, the Young modulus gets closer to the human skin average value as reported in literature (83 MPa) (Ni Annaidh, Bruyere, Destrade, Gilchrist, & Ottenio, 2012). The influence of OPU % was small on tensile strength and elongation at break, whereas it was remarkable on Young modulus. In particular, all films showed a strong increase of E at 0.5 % OPU content. This trend is more pronounced for 1:0.5 and 1:1 composition. The increase is attributed to the formation of ionic entanglements between residual amines on Ch and dicarboxylic acids of OPU extract, as already evidenced by FTIR and DSC analysis (Fig. 2 and Table 1). According to the scheme proposed in Fig. S6, such ionic interactions contribute to crosslinking, thus causing an increase in Young's modulus. In conclusion,

despite the low tensile strength values, the overall mechanical properties look adequate in view of possible applications as wound dressings.

3.5. Swelling study

It is well known that the release of drugs from hydrophilic crosslinked networks strongly depends on the swelling behavior. Swelling is strictly related to the physical structure, as the presence of a crosslinked network can significantly reduce the swelling ratio. Rate and duration of swelling were studied over a two-day period. Fig. 3 shows differences among the various Ch/diePEG hydrogel films loaded with 0.5 % OPU when placed in PBS solution. According to what reported in the literature (Berger et al., 2004), free chitosan shows higher swelling compared to covalently crosslinked chitosan hydrogels, since most of the amino groups of chitosan must have reacted with the crosslinker (Aly, 1998). Indeed, increasing the amount of crosslinker decreases the ability of chitosan to form hydrogen bonds with water molecules. Consequently, crosslinked films have a regular trend in PBS, with the 1:2 composition showing the lowest swelling ratio, in line with the higher crosslinking degree, whereas no appreciable differences are found between the other two compositions (Table 3). The equilibrium water content (EWC) represents the amounts of fluids that a material can absorb in relation to its weight. As for the swelling profiles, results revealed that EWC significantly decreased at increasing crosslinker content (Table 3). However, the EWC values of the Ch/diePEG films were only slightly larger than the per-cent water content values of the body (about 60 %). Thus, we can assume that such a similarity with the fluid contents of living tissues can increase the compatibility of these materials with the wound area. Taken together the observed results seem to be in line with the current literature on chemically crosslinked hydrogels films (Dogu & Okay, 2006; Gonzalez-Meijome et al., 2006; Mohammed, Ahmad, Ibrahim, & Zainuddin, 2018). This behavior can be explained by the simultaneous occurrence of two phenomena. The increase in diePEG content results in an increased crosslinking degree, which in turn causes restrained mobility of the macromolecular chains that hinders water penetration and brings about a depression in the swelling ratio. At the same time, the increasing number of crosslinks reduces the free volumes between the macromolecular chains, which then become less accessible to penetrant water molecules.

3.6. Water Vapor Transmission rate

The ability of a dressing to control water loss can be determined by WVTR. It is now well established that an extremely high WVTR may lead to the dehydration of a wound, whereas an unacceptably low WVTR may cause the accumulation of wound exudates (Hinman & Maibach, 1963; Queen, Gaylor, Evans, Courtney, & Reid, 1987; Winter, 1962). Thus, materials for wound healing applications are required to provide a moist environment able to support the natural healing process (Schunck, Neumann, & Proksch, 2005). The WVTR strictly depends on the characteristics of each wound dressings such as porosity, thickness, crosslink, *etc.*, which are derived from the material used and the preparation method. Accordingly to El Salmawi, suitable WVRT values for wound dressings are comprised in the range of 33–53 g/h•m_2 (El Salmawi, 2007). WVTR was examined for all film compositions, either unloaded or loaded with 0.5 % OPU (Table 4). WVRT values fell in the suitable range (around 44 g/h•m_2) for all the prepared Ch/diePEG films, indicating that the crosslinking process does not influence the diffusion of the water vapor in the film matrix. Conversely, the addition of OPU caused a decrease in WVRT. This outcome is probably due to the formation of strong macromolecular ionic entanglements caused by interactions of amines with dicarboxylic acids present in OPU extract, that slow down the diffusion of water vapor. This hypothesis is in agreement with the strong increase of Tg found by DSC analysis. Such an effect, however, is critical only in the case of pure chitosan, whose WVRT value fell out of the desirable range, whereas all the other films kept adequate WVRT values upon OPU addition.

3.7. Release study

Release kinetics of OPU from selected films was followed by UV spectroscopy. UV analysis allows to determine the concentration of low molecular weight components of OPU, which consist of a mixture of mono- and di-carboxylic phenolic acids (mainly piscidic and eucomic acids). According to the literature, phenolic derivatives absorb in the UV–vis range, and this technique is widely used for the quantification of phenolic compounds (Aleixandre-Tudo & du Toit, 2018). Conversely, the release of the high molecular weight fraction, consisting of polysaccharides, cannot be evidenced by UV analysis. However, as reported in a previous paper (Di Lorenzo et al., 2017), only the low molecular weight components of OPU are active in the wound healing process, and for this reason, we focus on them. To investigate the effect of different crosslinking degree on the release rate, films of the various Ch/PEG compositions loaded with the same amount of OPU (0.5 %) were tested and compared to the not crosslinked chitosan film. Cumulative OPU release (expressed as mg OPU/g film) is

reported in Fig. 4A. It is worth to notice how the release does not appears to be directly related to the swelling profile. Negligible differences were found between non-crosslinked chitosan and Ch/diePEG 1: 0.5 and 1:1, although the significant difference evidenced in their swelling ability. This interesting evidence may be explained by considering two competing mechanisms which determine the mobility of OPU molecules within the polymer matrix: diffusion through the network, driven by the water uptake and therefore related to the crosslinking density, and interaction with the amines of chitosan, which hampers the mobility. As shown in Fig. 3, the non-crosslinked chitosan films have a greater water absorption ability compared with the crosslinked hydrogel films, but at the same time it interacts more with OPU molecules, due to the higher number of free amines, thus slowing down the release and determining a release profile very close to those of Ch/diePEG 1:0.5 and 1:1. In the case of Ch/diePEG 1:2, the OPU release is significantly lower, presumably due to the more entangled polymer network which slows down the diffusion of OPU molecules, although their reduced interaction with chitosan. It is also worth of noting the fastest initial release shown by Ch/diePEG 1:0.5 compared to Ch and the other two compositions. The effect of the amount of loaded OPU was studied for 1:0.5 composition (Fig. 4B), which showed the best characteristics in terms of swelling and release properties. It is evident that release kinetics does not show a regular trend as a function of OPU loading. The final amount of OPU released is only slightly higher for the film with the higher OPU content (0.5 %) compared to the 0.1 % OPU film, whereas the release from OPU 0.25 % film is significantly lower. This result suggests that the release process is affected by OPU load; furthermore, at low OPU content (0.1 %) the film releases around 90 % of the initial cargo, whereas the release does not exceed 40–50 % in the case of films loaded with 0.25 and 0.5 % OPU.

3.8. Biological response: in vitro wound healing of HaCat in presence of OPU films

The use of a videomicroscopy time lapse station allowed to follow the evolution of gap closure in a HaCat monolayer, in the absence and the presence of films loaded with OPU. Based on the release study, the *in vitro* wound healing assay was performed on Ch/diePEG 1:0.5 formulation, both blank and loaded with the different OPU %. As shown in Fig. 5, all the films containing OPU are significantly fastening gap closure compared to both the untreated control and the wells treated with the unloaded Ch/diePEG film. The panel in Fig. 5a, which reports the photos of each selected field of view at different times, shows that the

films containing OPU seemed to fasten the scratch reparation process especially for the ones containing 0.1 and 0.25 % of OPU. A quantitative analysis (reported in Fig. 5b) has allowed to build the corresponding curve, where a higher rate of closure in case of keratinocytes monolayer treated with samples containing 0.1 % OPU, followed by 0.25 e 0.5 %, was found. For all the samples tested, the gap closure occurred within 20 h. Interestingly, the faster gap closure occurs when the Ch/diePEG films containing the lower amount of OPU (0.1 %) came in contact with the HaCat cells. The rate of cell migration in presence of OPU was about 3-fold higher compared to the rate in presence of the materials without OPU at 60 and 80 % of wound closure. This result was in accordance with the results obtained by Di Lorenzo et al., which used free OPU at a concentration of 0.1 % (Di Lorenzo et al., 2017). The best result obtained with a low amount of OPU was correlated to the complete release of OPU from the 0.1 % OPU film, as evidenced by release studies (Fig. 4b) and to the low pH value (3.86) of OPU aqueous solutions. High OPU concentrations, in fact, could have negative effects on wound closure, since could slightly modify the physiological pH of the cell medium. Therefore, the 0.1 % OPU concentration seems to be the optimal one. Moreover, from these data, we can also deduce that Ch/diePEG 1:0.5 films are not toxic and do not hamper the reparation in all the treatments.

4. Conclusion

OPU extracts have been known for a long time to accelerate skin injury repair and several evidences of their activity are already reported in literature. Here, a new formulation based on a PEG-crosslinked chitosan loaded with various amounts of OPU extract is presented as a wound healing activity. Three different PEG-chitosan formulations have been prepared and loaded with three different OPU amounts. Crosslinking of chitosan was successfully achieved by reaction with a low molecular weight diepoxy PEG, as confirmed by FTIR analysis and leaching tests. Overall, solid state characterization highlighted the establishment of physical and ionic interactions between chitosan and OPU. Tensile tests showed that the insertion of flexible PEG segments upon crosslinking caused a decrease of the Young′s modulus, which approaches the value of the human skin modulus. Swelling characteristics, water vapor transmission rate and release kinetics demonstrated that the films are appropriate for the proposed application. Finally, the results of a scratch test on HaCat cellular monolayer performed in presence of Ch/DiePEG 1:0.5 film showed that the film itself does not hinder the natural healing process, indeed loading with OPU results in an

activity of the film in the wound repair process, especially for the sample with the lowest OPU content (0.1 %).

Funding

This work was partly supported in the frame of National Operative Program (PON 03PE_00060_3, BioScience)

CRediT authorship contribution statement

O. Catanzano: Methodology, Formal analysis, Investigation, Writing - review & editing. **G. Gomez d'Ayala:** Investigation, Validation, Writing - review & editing. **A. D'Agostino:** Investigation, Validation. **F. Di Lorenzo:** Writing - review & editing. **C. Schiraldi:** Supervision, Writing - review & editing. **M. Malinconico:** Funding acquisition, Supervision. **R. Lanzetta:** Supervision. **F. Bonina:** Resources, Supervision. **P. Laurienzo:** Conceptualization, Supervision, Writing - original draft.

Appendix A. Supplementary data

Supplementary material related to this article can be found, in the online version, at doi:https://doi.org/10.1016/j.carbpol.2021.117987.

References

Aleixandre-Tudo, J. L., & du Toit, W. (2018). The role of UV-visible spectroscopy for phenolic compounds quantification in winemaking. In R. L. Solís-Oviedo, & ´A. de la Cruz Pech-Canul (Eds.), Frontiers and new trends in the science of fermented food and beverages. IntechOpen. https://doi.org/10.5772/intechopen.79550.

Aly, A. S. (1998). Self-dissolving chitosan, I. Preparation, characterization and evaluation for drug delivery system. Die Angewandte Makromolekulare Chemie, 259(1), 13–18.

Archana, D., Singh, B. K., Dutta, J., & Dutta, P. K. (2013). In vivo evaluation of chitosan-PVP-titanium dioxide nanocomposite as wound dressing material. Carbohydrate Polymers, 95(1), 530–539.

ASTM-International. (2013). D1653-13 standard test methods for water vapor transmission of organic coating films. West Conshohocken, PA: ASTM International.

Berger, J., Reist, M., Mayer, J. M., Felt, O., Peppas, N. A., & Gurny, R. (2004). Structure and interactions in covalently and ionically crosslinked chitosan hydrogels for biomedical applications. European Journal of Pharmaceutics and Biopharmaceutics, 57 (1), 19–34.

Boateng, J., & Catanzano, O. (2015). Advanced therapeutic dressings for effective wound healing–A review. Journal of Pharmaceutical Science, 104(11), 3653–3680.

Boateng, J. S., Matthews, K. H., Stevens, H. N., & Eccleston, G. M. (2008). Wound healing dressings and drug delivery systems: A review. Journal of Pharmaceutical Science, 97 (8), 2892–2923.

Chen, S. L., Fu, R. H., Liao, S. F., Liu, S. P., Lin, S. Z., & Wang, Y. C. (2018). A PEG-Based hydrogel for effective wound care management. Cell Transplantation, 27(2), 275–284.

Christina, B., Taylor, L. S., & Mauer, L. J. (2015). Physical stability of l-ascorbic acid amorphous solid dispersions in different polymers: A study of polymer crystallization inhibitor properties. Food Research International, 76(Pt 3), 867–877.

D'Agostino, A., Maritato, R., La Gatta, A., Fusco, A., Reale, S., Stellavato, A., … Schiraldi, C. (2019). In vitro evaluation of novel hybrid cooperative complexes in a wound healing model: A step toward improved bioreparation. International Journal of Molecular Science, 20(19).

Di Lorenzo, F., Silipo, A., Molinaro, A., Parrilli, M., Schiraldi, C., D'Agostino, A., & Lanzetta, R. (2017). The polysaccharide and low molecular weight components of Opuntia ficus indica cladodes: Structure and skin repairing properties. Carbohydrate Polymers, 157, 128–136.

Dogu, Y., & Okay, O. (2006). Swelling–deswelling kinetics of poly(Nisopropylacrylamide) hydrogels formed in PEG solutions. Journal of Applied Polymer Science, 99(1), 37–44.

Dong, Y. M., Ruan, Y. H., Wang, H. W., Zhao, Y. G., & Bi, D. X. (2004). Studies on glass transition temperature of chitosan with four techniques. Journal of Applied Polymer Science, 93(4), 1553–1558.

El Salmawi, K. M. (2007). Gamma radiation-induced crosslinked PVA/Chitosan blends for wound dressing. Journal of Macromolecular Science Part A- Pure and Applied Chemistry, 44(5), 541–545.

Elgadir, M. A., Uddin, M. S., Ferdosh, S., Adam, A., Chowdhury, A. J. K., & Sarker, M. Z. I. (2015). Impact of chitosan composites and chitosan nanoparticle composites on various drug delivery systems: A review. Journal of Food and Drug Analysis, 23(4), 619–629.

Fang, Q., Huang, C., You, C., & Ma, S. (2015). Opuntia extract reduces scar formation in rabbit ear model: A randomized controlled study. International Journal of Low Extremity Wounds, 14(4), 343–352.

Gonzalez-Meijome, J. M., Lira, M., Lopez-Alemany, A., Almeida, J. B., Parafita, M. A., & Refojo, M. F. (2006). Refractive index and equilibrium water content of conventional and silicone hydrogel contact lenses. Ophthalmic and Physiological Optics, 26(1), 57–64.

Hinman, C. D., & Maibach, H. (1963). Effect of air exposure and occlusion on experimental human skin wounds. Nature, 200, 377–378.

Ivanova, B., & Spiteller, M. (2010). Salts of aromatic amines: Crystal structures, spectroscopic and non-linear optical properties. Spectrochimica Acta A Molecular and Biomolecular Spectroscopy, 77(4), 849–855.

Ivanova, E. P., Bazaka, K., & Crawford, R. J. (2014). 3 - Advanced synthetic polymer biomaterials derived from organic sources. In E. P. Ivanova, K. Bazaka, & R. J. Crawford (Eds.), New functional biomaterials for medicine and healthcare (pp. 71–99). Woodhead Publishing.

Kiuchi, H., Kai, W., & Inoue, Y. (2008). Preparation and characterization of poly (ethylene glycol) crosslinked chitosan films. Journal of Applied Polymer Science, 107 (6), 3823–3830.

Krauklis, A. E., & Echtermeyer, A. T. (2018). Mechanism of yellowing: Carbonyl formation during hygrothermal aging in a common amine epoxy. Polymers, 10(9).

Matica, M. A., Aachmann, F. L., Tondervik, A., Sletta, H., & Ostafe, V. (2019). Chitosan as a wound dressing starting material: Antimicrobial properties and mode of action. International Journal of Molecular Science, 20(23).

Mengatto, L. N., Helbling, I. M., & Luna, J. A. (2012). Recent advances in chitosan films for controlled release of drugs. Recent Patents on Drug Delivery & Formulation, 6(2), 156–170.

Mohammed, A. H., Ahmad, M. B., Ibrahim, N. A., & Zainuddin, N. (2018). Effect of crosslinking concentration on properties of 3-(trimethoxysilyl) propyl methacrylate/ N-vinyl pyrrolidone gels. Chemistry Central Journal, 12(1), 15.

Ni Annaidh, A., Bruyere, K., Destrade, M., Gilchrist, M. D., & Ottenio, M. (2012). Characterization of the anisotropic mechanical properties of excised human skin. Journal of the Mechanical Behavior of Biomedical Materials, 5(1), 139–148.

Oyatogun, G. M., Esan, T. A., Akpan, E. I., Adeosun, S. O., Popoola, A. P. I., Imasogie, B. I., & Akinluwade, K. J. (2020). Chapter 11 - Chitin, chitosan, marine to market. In S. Gopi, S. Thomas, & A. Pius (Eds.), Handbook of chitin and chitosan (pp. 341–381). Elsevier.

Panico, A. M., Cardile, V., Garufi, F., Puglia, C., Bonina, F., & Ronsisvalle, S. (2007). Effect of hyaluronic acid and polysaccharides from Opuntia ficus indica (L.) cladodes on the metabolism of human chondrocyte cultures. Journal of Ethnopharmacology, 111(2), 315–321.

Queen, D., Gaylor, J. D., Evans, J. H., Courtney, J. M., & Reid, W. H. (1987). Evaluation of gaseous transmission (O2 and CO2) through burn wound dressings. Burns, Including Thermal Injuries, 13(5), 357–364.

Rocchetti, G., Pellizzoni, M., Montesano, D., & Lucini, L. (2018). Italian Opuntia ficusindica Cladodes as rich source of bioactive compounds with health-promoting properties. Foods, 7(2).

Rossi, S., Marciello, M., Sandri, G., Ferrari, F., Bonferoni, M. C., Papetti, A., … Grisoli, P. (2007). Wound dressings based on chitosans and hyaluronic acid for the release of

chlorhexidine diacetate in skin ulcer therapy. Pharmaceutical Development and Technology, 12(4), 415–422.

Schunck, M., Neumann, C., & Proksch, E. (2005). Artificial barrier repair in wounds by semi-occlusive foils reduced wound contraction and enhanced cell migration and reepithelization in mouse skin. Journal of Investive Dermatology, 125(5), 1063–1071.

Straccia, M. C., Gomez d'Ayala, G., Romano, I., Oliva, A., & Laurienzo, P. (2015). Alginate hydrogels coated with chitosan for wound dressing. Marine Drugs, 13(5), 2890–2908.

Szymanska, E., & Winnicka, K. (2015). Stability of chitosan-a challenge for pharmaceutical and biomedical applications. Marine Drugs, 13(4), 1819–1846.

Tanuma, H., Kiuchi, H., Kai, W., Yazawa, K., & Inoue, Y. (2009). Characterization and enzymatic degradation of PEG-cross-linked chitosan hydrogel films. Journal of Applied Polymer Science, 114(3), 1902–1907.

Tanuma, H., Saito, T., Nishikawa, K., Dong, T., Yazawa, K., & Inoue, Y. (2010). Preparation and characterization of PEG-cross-linked chitosan hydrogel films with controllable swelling and enzymatic degradation behavior. Carbohydrate Polymers, 80(1), 260–265.

Thomas, S., & Uzun, M. (2019). 2 - Testing dressings and wound management materials. In S. Rajendran (Ed.), Advanced textiles for wound care (second edition, pp. 23–54). Woodhead Publishing.

Trombetta, D., Puglia, C., Perri, D., Licata, A., Pergolizzi, S., Lauriano, E. R., & Bonina, F. P. (2006). Effect of polysaccharides from Opuntia ficus-indica (L.) cladodes on the healing of dermal wounds in the rat. Phytomedicine, 13(5), 352–358.

Wang, L., Khor, E., Wee, A., & Lim, L. Y. (2002). Chitosan-alginate PEC membrane as a wound dressing: Assessment of incisional wound healing. Journal of Biomedical Materials Research, 63(5), 610–618.

Winter, G. D. (1962). Formation of the scab and the rate of epithelization of superficial wounds in the skin of the young domestic pig. Nature, 193, 293–294.

Yang, J., Tian, F., Wang, Z., Wang, Q., Zeng, Y. J., & Chen, S. Q. (2008). Effect of chitosan molecular weight and deacetylation degree on hemostasis. Journal of Biomedical Materials Research B Applied Biomaterials, 84(1), 131–137.

Tables and figures

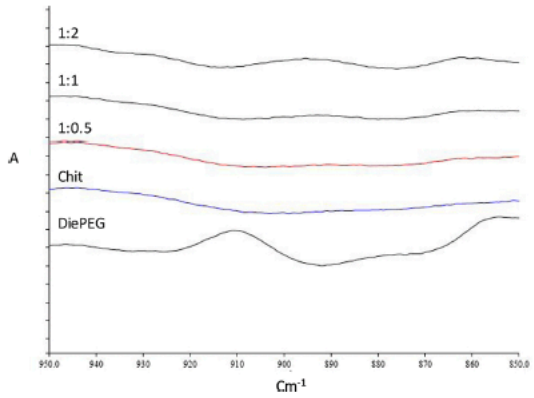

Sample	Weight loss (%)
Ch/diePEG 1:0.5	1.9 ± 0.2
Ch/diePEG 1:1	1.5 ± 0.3
Ch/diePEG 1:2	1.5 ± 1.1

Fig. 1. FTIR spectra (absorbance) of diePEG, Ch and Ch/diePEG films in the range 950 - 850 cm^{-1}; weight loss (%) after leaching with water of crosslinked films (% refers to the total amount of initial diePEG).

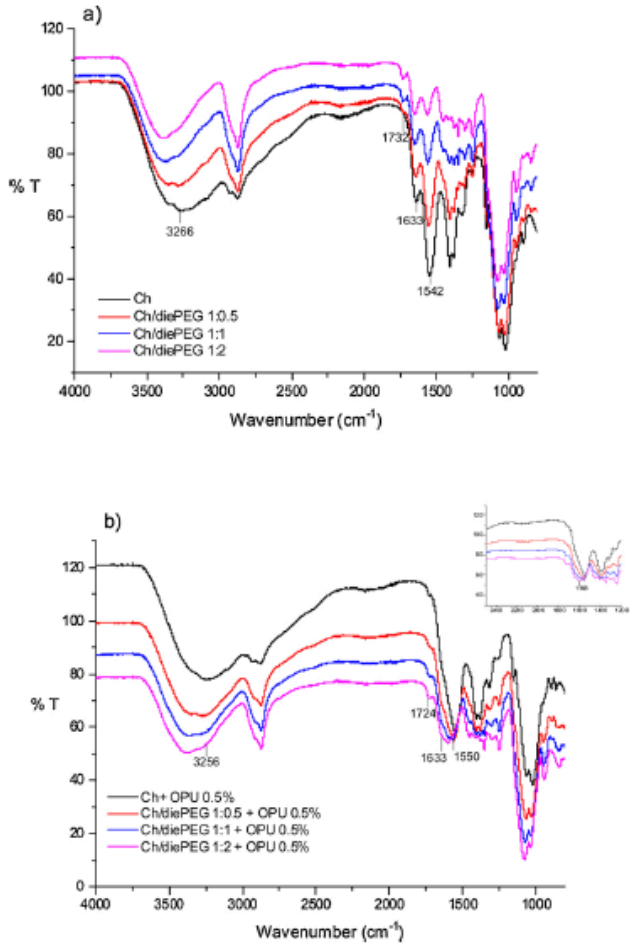

Fig. 2. a) FTIR spectra of Ch and Ch/diePEG films; b) FTIR spectra of Ch and Ch/diePEG films loaded with 0.5 % OPU.

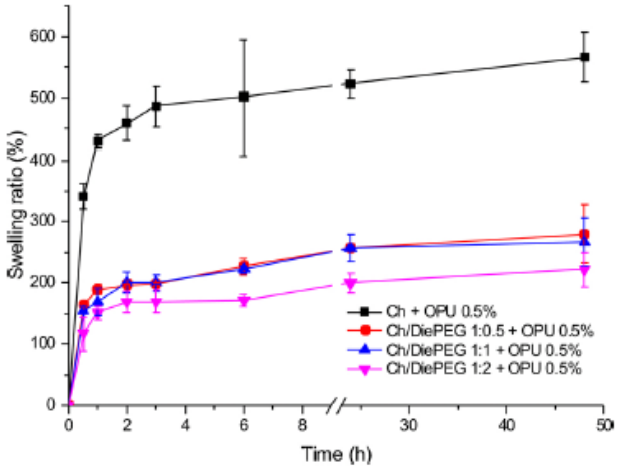

Fig. 3. Swelling profiles of Ch/diePEG films loaded with OPU 0.5 % at different Ch-diePEG ratio in PBS.

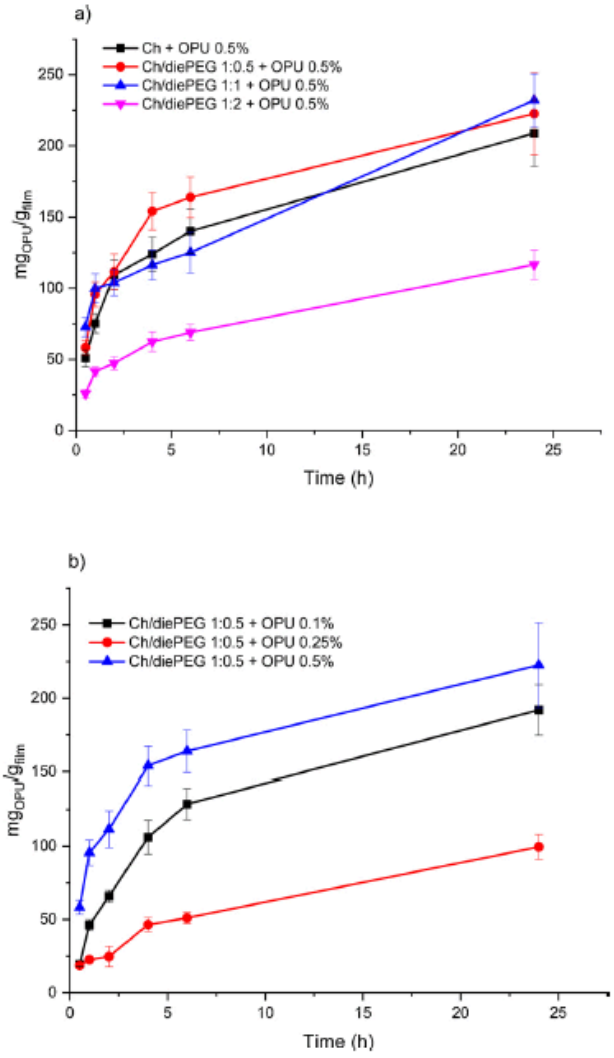

Fig. 4. a) Cumulative release profiles of OPU from the various Ch/diePEG films with 0.5 % OPU. b) Cumulative release profiles of OPU from Ch/diePEG 1:0.5 film with different OPU %.

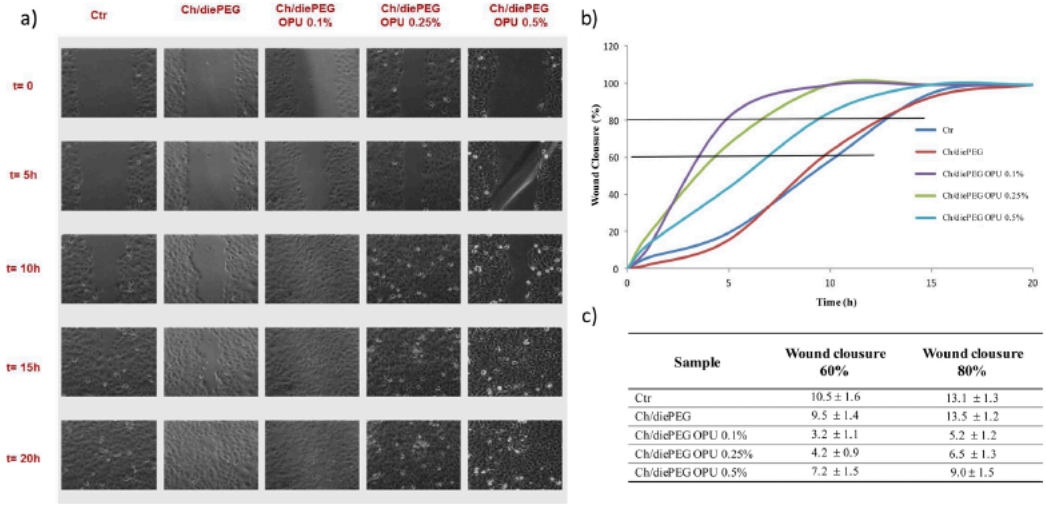

Sample	Wound clousure 60%	Wound clousure 80%
Ctr	10.5 ± 1.6	13.1 ± 1.3
Ch/diePEG	9.5 ± 1.4	13.5 ± 1.2
Ch/diePEG OPU 0.1%	3.2 ± 1.1	5.2 ± 1.2
Ch/diePEG OPU 0.25%	4.2 ± 0.9	6.5 ± 1.3
Ch/diePEG OPU 0.5%	7.2 ± 1.5	9.0 ± 1.5

Fig. 5. a) Representative panel of scratch assay in the control and in the presence of Ch/diePEG 1:0.5 films (magnification 100X); b) Relative curves of wound closure (%) *vs.* time (h) calculating the wound closure of at least 5 fields of view for each sample; c) Healing time, extrapolated from the curves, at 60 and 80 % of wound closure.

Table 1
Glass transition (Tg), melting temperature (Tm) and moisture content (MC) of the films with different Ch/diePEG ratio and OPU contents.

Sample	Tg (°C)	Tm (°C)	MC (%)
Ch	145	–	20.7
OPU (powder)	92	173	–
Ch + OPU 0.1 %	143	–	–
Ch + OPU 0.25 %	141	–	–
Ch + OPU 0.5 %	142	173	11.7
Ch/diePEG 1:0.5	135	–	7.0
Ch/diePEG 1:0.5 + OPU 0.1 %	136	–	–
Ch/diePEG 1:0.5 + OPU 0.25 %	139	–	–
Ch/diePEG 1:0.5 + OPU 0.5 %	140	–	10.8
Ch/diePEG 1:1	136	–	6.8
Ch/diePEG 1:1 + OPU 0.1 %	136	–	–
Ch/diePEG 1:1 + OPU 0.25 %	137	–	–
Ch/diePEG 1:1 + OPU 0.5 %	140	–	12.7
Ch/diePEG 1:2	156	–	2.3
Ch/diePEG 1:2 + OPU 0.1 %	156	–	–
Ch/diePEG 1:2 + OPU 0.25 %	156	–	–
Ch/diePEG 1:2 + OPU 0.5 %	158	–	9.0

Table 2
Strength at break (σ_B), Elongation at break (ε_B), and Young's modulus (E) of OPU-loaded crosslinked films and Ch + OPU 0.5 % film. Each value represents the mean ± SD of triplicate determination in three independent experiments.

Sample	σ_B (MPa) ± S.D.	ε_B (%) ± S.D.	E (MPa) ± S.D.
Ch + OPU 0.5 %	9.4 ± 1.6	6.1 ± 1.9	3418.0 ± 430.4
Ch/diePEG 1:0.5 + OPU 0.1 %	18.1 ± 5.9	42.6 ± 11.7	789.3 ± 91.4
Ch/diePEG 1:0.5 + OPU 0.25 %	11.6 ± 3.8	22.3 ± 2.7	754.7 ± 102.5
Ch/diePEG 1:0. 5 + OPU 0.5 %	8.0 ± 0.8	22.2 ± 2.0	1445.0 ± 96.4
Ch/diePEG 1:1 + OPU 0.1 %	13.0 ± 3.1	46.89 ± 3.2	30.9 ± 1.2
Ch/diePEG 1:1 + OPU 0.25 %	14.4 ± 3.4	56.2 ± 2.0	25.6 ± 2.5
Ch/diePEG 1:1 + OPU 0.5 %	4.4 ± 0.9	36.9 ± 2.6	331.2 ± 12.1
Ch/diePEG 1:2 + OPU 0.1 %	5.8 ± 0.8	54.6 ± 2.0	1.0 ± 0.2
Ch/diePEG 1:2 + OPU 0.25 %	6.0 ± 1.1	55.9 ± 4.9	9.9 ± 0.4
Ch/diePEG 1:2 + OPU 0.5 %	5.5 ± 0.5	72.6 ± 2.6	19.1 ± 2.1

Table 3
Swelling parameters in PBS for the various Ch/diePEG films loaded with OPU.0.5 %.

Sample	EWC (%) ± S.D.	Swelling ratio (%) ± S.D.
Ch + OPU 0.5 %	85.3 ± 2.4	522.7 ± 22.7
Ch/diePEG 1:0.5 + OPU 0.5 %	72.0 ± 1.7	257.8 ± 22.5
Ch/diePEG 1:1 + OPU 0.5 %	72.5 ± 1.6	257.4 ± 22.5
Ch/diePEG 1:2 + OPU 0.5 %	66.6 ± 1.9	200.0 ± 16.8

Table 4
Results of WVTR measurements [$g\ /hm^{-2}$] for all compositions, either unloaded or loaded with 0.5 % OPU. Values are expressed as the average of three independent experiments with a SD ± 3.0 %.

Sample	WVTR Unloaded films	WVTR + OPU 0.5 %
Ch	44.0	26.8
Ch/diePEG 1:0.5	44.1	37.6
Ch/diePEG 1:1	44.5	43.2
Ch/diePEG 1:2	43.2	39.1